NANO LETTERS

2001
Vol. 1, No. 6
319−322

Seed Mediated Formation of Bimetallic Nanoparticles by UV Irradiation: A Photochemical Approach for the Preparation of “Core–Shell” Type Structures

Kaushik Mallik, Madhuri Mandal, Narayan Pradhan, and Tarasankar Pal*

Department of Chemistry, Indian Institute of Technology, Kharagpur 721 302, India

Received April 14, 2001 *(Revised Manuscript Received May 24, 2001)*

ABSTRACT

Bimetallic gold and silver particles, a core–shell type structure, have been prepared by a UV-photoactivation technique. The optical absorption spectra are recorded and compared with various absorption profiles due to Au–Ag particles described in the literature. Initially Au particles formed by UV irradiation, which act as the seed particles, catalyzed the reduction of added silver ion in the presence of UV light to yield bimetallic (Au_{core}–Ag_{shell}) particles. Preferential dissolution of Au particles by cyanide and TEM images of the particles corroborates the “core–shell” type configuration.

Metal nanoparticles, composed of two (or more) different elements, are of interest from both technological and scientific points of view for improving catalytic activity and properties. Preparation of bimetallic nanoparticles from metal salts can be divided into two groups: coreduction and successive reduction of two metal salts. Coreduction is the simple preparative method of bimetallic nanoparticles; the method is used in the preparation of monometallic nanoparticles. The only difference is the number of metal precursor ions. Successive reduction is usually carried out to prepare “core−shell”-structured bimetallic nanoparticles. The deposition of one metal on a preformed monometallic nanoparticle of another metal seems to be very effective. For this purpose, however, a second metal must be deposited on the surface of the preformed particles, and the preformed monometallic nanoparticles should be chemically surrounded by the deposited element.

Ag−Au alloys were prepared in Laponite suspensions[1] and in ethanol solution containing poly(*N*-vinyl-2-pyrrolidone).[2] Simultaneous coreduction of $AgNO_3$ and $HAuCl_4$ with sodium citrate was also used for the synthesis of Ag−Au alloys.[3]

A bilayered Au_{core}−Ag_{shell} cluster[4] was obtained by mixing a solution of $KAuCl_4$ and Ag_2SO_4 in the presence of PVA at the dose rate of 3.8 kGy h^{-1}. In an another interesting study, the formation of bilayered Ag_{core}−Au_{shell} clusters is obtained if the precursors are gold and silver cyanide, where gold behaves as the less noble metal.[5] Schmid[6] et al. reduced $PtCl_6^{2-}$ in an aqueous gold sol by hydroxylamine; they obtained particles consisting of an 18 nm gold core surrounded by platinum crystals of about 5 nm. In a very recent study, Henglein[7] prepared Au_{core}−Pt_{shell} and Pt_{core}–Au_{shell} type colloidal nanoparticles by using γ-radiation from a source of ^{60}Co.

This communication reports for the first time a photochemical approach (UV irradiation) for the preparation of seed mediated bimetallic nanoparticles, having “core−shell” type structure. It has been proved that the deposition of one less noble metal (M) “shell” on a preformed nanoparticle of another more noble metal “core” (M*) seems to be very effective by UV activation.

Triton X-100 (chemically known as poly(oxyethylene)-*iso*-octylphenylether and abbreviated as TX-100), $HAuCl_4$, and $AgNO_3$ were purchased from Aldrich. Double-distilled water was used throughout the experiment. Photochemical reactions were carried out in 1-cm quartz cuvettes. The cuvette filled with solution was placed horizontally for UV irradiation under a portable germicidal lamp (15 W; G 15 T8 UV−C, Phillips, Holland) at a distance of 10 cm.

UV−visible spectra were measured in Shimadzu UV-160 digital spectrophotometer (Kyoto, Japan) with 1-cm quartz cuvette. Transmission electron microscopy (TEM) studies of the particles were carried out at 200 kV using a Hitachi HF-2000 TEM equipped with a field emission source. An energy-dispersive X-ray spectrometer (EDS) attached to the Hitachi HF-2000 TEM was used to determine the chemical

10.1021/nl0100264 CCC: $20.00

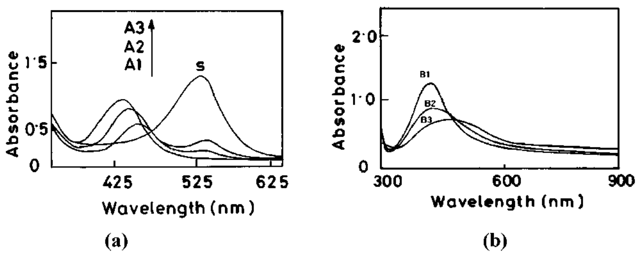

(a) (b)

Figure 1. (a) Absorption spectra of Au particles in solution produced by UV radiation of deaerated solution containing TX-100 (10^{-2} M) and $HAuCl_4$ (5.0×10^{-3} M), of which the final concentration of Au(III) ion remains 5.0×10^{-4} M. After 20-min irradiation, the solution turned pink and showed a plasmon absorption band at 520 nm ($\lambda_{max} = 520$ nm), indicating the formation of gold particles, i.e., Au(0). These particles were used as the seed (S) for further enlargement. A plasmon band was obtained on photoactivation of the solution containing [Au(0)] + [$AgNO_3$]. The overall particle concentration in the solution was 5.0×10^{-4} M. Final concentrations of metal sol and silver ion were adjusted to 1.67×10^{-4} and 3.33×10^{-4} M, respectively, in TX-100 medium. After 10-min irradiation, the pink colored solution turned brown and the plasmon absorption band shifted to 450 nm ($\lambda_{max} = 450$ nm, Figure 1a; A1). Irradiation for another 15 min shifted the absorption band to 440 nm (A2), and after prolonged irradiation, the adsorption band was fixed at 435 nm (A3) and the solution was golden brown, indicating of the formation of silver particles on the gold seeds (S_1). (b) In another set of experiments, final concentration of metal sol (S_1) and silver ion were adjusted to 5×10^{-5} and 4.5×10^{-4} M, respectively, in TX-100 medium. Overall particle concentration in this mixture, i.e., [S_1] + [$AgNO_3$], was 5.0×10^{-4} M. With increasing irradiation time, a set of broad plasmon adsorption bands B1, B2, B3 indicates gradual enlargement of the particles.

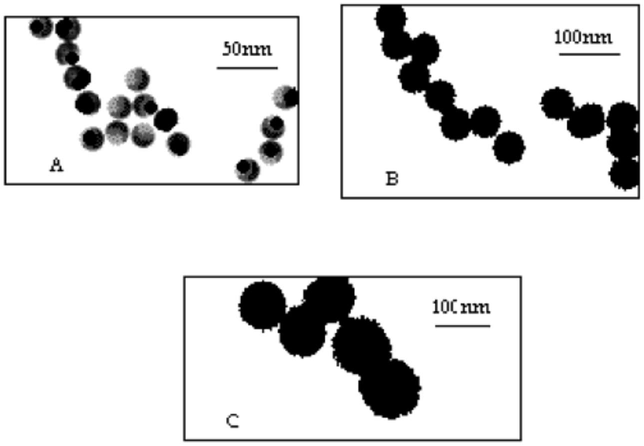

Figure 2. Transmission electron micrograph (TEM). TX-100 (0.01M) and $HAuCl_4$ (0.005M) were placed in a quartz cuvette so that the final concentration of Au(III) ion remained 5.0×10^{-4} M. After 20-min irradiation under the UV light, the solution turned pink. TEM specimens were prepared by placing microdrops of colloid solution on a carbon film supported by copper grids. A TEM image showed that the gold particles have a diameter of ~20 nm (A). In the second step, the final concentration of metal sol and silver ion were adjusted to 1.67×10^{-4} and 3.33×10^{-4} M, respectively, in TX-100 medium. The overall particle concentration in this mixture, i.e., [Au(0)] + [$AgNO_3$] was 5.0×10^{-4} M. After prolonged UV irradiation, the peak of plasmon adsorption band was fixed at 435 nm and TEM images (~60 nm) (B) reflect the formation of silver layer on the gold seeds, i.e., $Au_{core}-Ag_{shell}$ (S_1). In S_1, a single layer of silver was on Au_{core}. For the attachment of another layer of silver on $Au_{core}-Ag_{shell,}$ the final concentrations of metal sol (S_1) and silver ion were adjusted to 5×10^{-5} and 4.5×10^{-4} M, respectively, in TX-100 medium. Overall particle concentration in this mixture, i.e., [S_1] + [$AgNO_3$], was 5.0×10^{-4} M. After prolonged UV irradiation, the TEM images (~100 nm) (C) reflect the formation of another layer of silver particles on $Au_{core}-Ag_{shell}$ (S_2).

composition of the samples. TEM specimens were prepared by placing microdrops of colloid solution on a carbon film supported by copper grids.

For the preparation of gold seeds (S), TX-100 (10^{-2} M) and $HAuCl_4$ (5.0×10^{-3} M) were taken in a quartz cuvette so that the final concentration of Au(III) ion remained 5.0×10^{-4} M. Then the cuvette was placed directly under the UV light source. After 20-min irradiation, the solution turned pink and showed a plasmon absorption band at 523 nm ($\lambda_{max} = 523$ nm, Figure 1a., S), indicating the formation of gold particles. These particles were used as the seed (S) for further enlargement. In the absence of gold particles (initially), i.e., during seed formation, there existed an induction period for the formation of the seed particles. A TEM image showed that the particle diameter lies within the range ~20 nm (Figure 2 A).

Two sets of solutions (S_1 and S_2) were prepared by using the following procedure. In the first step of particle enlargement for the preparation of S_1, seed particles (S) were used for their further growth. Final concentrations of metal sol and silver ion were adjusted to 1.67×10^{-4} and 3.33×10^{-4} M, respectively, in TX-100 medium. The overall particle concentration in this mixture, i.e., [Au(0)] + [$AgNO_3$] was 5.0×10^{-4} M. Next the solution was taken in a quartz cuvette and placed directly under UV light source. After 10-min irradiation, the pink colored solution turned brown and the plasmon absorption band shifted to 450 nm ($\lambda_{max} = 450$ nm, Figure 1a, A1). After irradiation for another 15 min, the absorption band shifted to 440 nm (Figure 1a., A2) Prolonged irradiation resulted in an absorption band fixed at 435 nm (Figure 1a., A3) and a golden brown appearance of the solution was an indication of the formation of silver particles presumably on the gold seeds, i.e., $Au_{core}-Ag_{shell}$. With irradiation of a mixture of gold seed and Ag(I) for longer time or increasing the UV light flux density, the plasmon peak shifted toward the blue region. The blue shift has been attributed due to the progressive covering of Au particle by silver layers. Due to the Ag covered Au, the plasmon band was Ag dominated. TEM image showed that the average particle size was ~60 nm (Figure 2, B). It was observed that silver ions were reduced catalytically in the presence of gold seed particles, as it happens in photography during incipient image formation.

For the preparation of S_2, S_1 was used as the seed particle, which has silver-coated gold particles. The final concentration of metal sol and silver ion were adjusted to 5×10^{-5} and 4.5×10^{-4} M, respectively, in the TX-100 medium. Overall particle concentration in this mixture, i.e., [S_1] + [$AgNO_3$], was 5.0×10^{-4} M. Successive irradiation resulted in gradual thickening of the silver layer onto the S_1 particles. This was reflected in the successive red-shifted (peaks changing from 438 nm to 450 nm) UV−visible spectra

(Figure 1b). Similar red-shifted spectra were also obtained when different but higher amounts of Ag(I) (1×10^{-4} to 2.5×10^{-4}M) were added to a fixed amount of S_1 (1.25×10^{-5} M) and irradiated for 10 min. Broad plasmon absorption bands indicated further enlargement of the particles (Figure 1b, B1, B2, B3). The solution, when viewed through transmitted light, appeared brown with a yellow tinge. It appeared faint yellow when viewed perpendicularly. The particles were rather unstable; they were agglomerated and subsequently precipitated just after an hour of removal from the UV source. A representative TEM image for the B3 (full grown particle) shows that the average particle diameter was ~100 nm (Figure 2, C).

We developed a general and reproducible photochemical technique for the preparation and growth of gold–silver bimetallic nanoparticles having the configuration Au_{core}–Ag_{shell}. First, we prepared smaller metal particles, then we used them as seeds or nucleation centers for the preparation of desired bimetallic particles with larger dimension.

In this paper, nanosized gold particles prepared by UV irradiation method[8] and with better monodispersity were used as seed particles. In the second step, the required amount of metal seed (Au) particles, metal salt ($AgNO_3$), and TX-100 (playing roles of both reducing agent and particle stabilizer) were mixed and kept under UV light. At this stage, the preformed seeds act as nucleation centers and become larger due to the reduction of the added bulk metal ions onto the surface of the seeds.

The recommended mechanism suggests a two-step process, i.e., nucleation and the successive growth of the particles. In the first step, metal ions in solution are reduced. The atoms thus produced agglomerate to form small clusters. The nanoclusters thus formed act as nucleation centers and catalyze the reduction process of the remaining metal ions present in the bulk. The result is the autocatalytic growth of the nucleation centers addressed as “development”. Current studies reveal further that the reduction potentials of $metal_{ion}/metal_{atom}$ and $metal_{ion}/metal_{particle}$ systems become more negative compared to those of the corresponding bulk metal.[9–13] For example, the reduction potential of the $Au^{III}/Au_{metal\ (aqueous)}$ system is +1.5 V versus NHE. But for the $Au^{III}/Au_{atom\ (aqueous)}$ system it is −1.5V and for $Au^{III}_{(aqueous)}/Au_{cluster}$ system the reduction potential has an intermediate value. This result has a great significance in understanding the mechanism of particle synthesis. The formation of metal atoms from its ions is very difficult because of the large negative potential of the $metal_{ion\ (aqueous)}/metal_{atom}$ system. Often impurities act as nucleation centers, as they generally increase the reduction potential of $metal_{ion\ (aqueous)}/metal_{atom}$ system, causing a favorable metal ion reduction.[14] Once the nucleation center is created, it acts as a catalyst for the reduction of remaining metal ions, if present in the solution. In this case, photoactivation did produce Au particles each time, but no Ag particles could be produced if $HAuCl_4$ replaced $AgNO_3$ in TX-100.

If metal ions (M^{*+}) of different salts are added, then they are adsorbed on the surface of the metal cluster (M) and on reduction of the metal ions by a suitable environment, formation of monolayer of metal similar to the M_{core}–M^*_{shell} structure (Scheme 1) may be possible. In this way, a series of M* layers can be formed onto the seed particles by the controlled supply and reduction of M^{*+}, i.e., the sizes of the bimetallic particles were controlled by varying the ratio of seed to that of the added metal ions.

Scheme 1

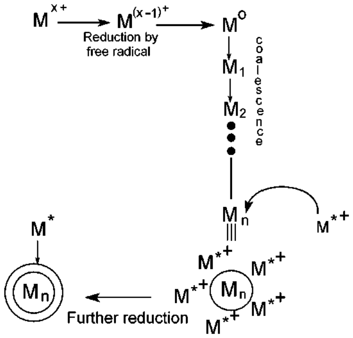

Further confirmation of the core–shell (Au_{core}–Ag_{shell}) structure was authenticated from the well-known cyanide-dependent dissolution of the Ag layers under ambient condition. The successive changes (decrease and shift) of the absorbance of the plasmon band at $\lambda_{max} \sim 435$ nm (due to the surface oscillation of the electron gas, whereas discrete electronic excitation due to interband transition occurs at shorter wavelength for Ag in the UV as well as visible spectra) during dissolution by cyanide also lends support to the core–shell structure. Repeated photoactivation of different mixtures of gold seed particles, Au(0) and $AgNO_3$, has been done. With the higher amounts of Ag(I) ion (10 to 100 times excess), gold seed particles were covered with Ag layers after 10 min of photoactivation. The peak position remained in the 435 nm region. However, 1-fold excess amount of Ag(I) ion (in comparison to gold seed) could not cover the gold seed particles completely, and hence the plasmon bands due to gold became evident at ~525 nm region along with the silver band at ~435 nm. The partially covered gold particles showed a double-hump, similar to the one that is obtained from a mixture of Ag and Au particles. Successive addition of Ag(I) ion followed by photoactivation transformed the double-hump curve of the partially covered gold particles into a curve having only one peak ($\lambda_{max} \sim 435$ nm), due the to core–shell structure. Larger amount of Ag(I) ion (100 times excess) and a shorter time of photoirradiation (1−2 min) also produced a double-hump curve (Figure 3b). The double-hump curve changed into a curve with single maxima on repetitive photoactivation (Figure 3c). Apparently the curve seemed to be the silver plasmon band, but it was nothing but the core–shell structure. This indicates the progressive covering of seed particles. The fully covered Au particles did not show any hump in the 525 nm region, instead the plasmon band due to the core–shell structure obtained reflects the true Ag plasmon band as if there was no Au in the medium (Figure 3). The preferential gold particle dissolution of the core–shell or the partially covered gold particles was always observed with cyanide under ambient conditions. This could be best visualized for a

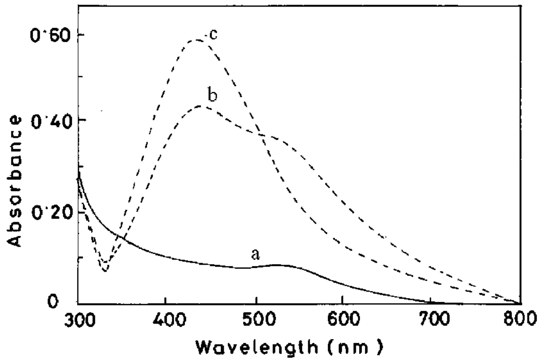

Figure 3. UV−visible spectra of (a) gold seed (S), (b) partially covered gold seed, and (c) core−shell structure in TX-100 (10^{-2}M) medium. Conditions: (a) [gold seed] = 1.25×10^{-5} M; (b) [gold seed] = 1.25×10^{-5} M and [$AgNO_3$] = 2.5×10^{-4} M, irradiation time 2 min; (c) [gold seed] = 1.25×10^{-5} M and [$AgNO_3$] = 2.5×10^{-4} M, irradiation time 10 min.

solution with partially covered gold particles (double hump). The core−shell structure dissolved in cyanide, and the kinetics of the dissolution is discussed elsewhere.[15] Both the solutions (core−shell and the partially covered gold particles) remained stable for about 1 h.

Energy deposition throughout the solution ensures the homogeneous distribution of photolytic radicals formed by excitation and ionization of the solvent. However, direct photolysis of H_2O is UV light source dependent.

$$H_2O \xrightarrow{h\nu} H^\bullet + OH^\bullet$$

R−OCH_2CH_2−OH [R = $(CH_3)_3CCH_2C(CH_3)_2C_6H_4(OCH_2CH_2)_{\sim 9}$−] is the scavenger of $H^\bullet$ and $OH^\bullet$ radicals. TX-100 on oxidation by $H^\bullet/OH^\bullet$ yields R−$OCH_2CH^\bullet$−OH, which has strong reducing property as H atoms. On the other hand, it is known that photolysis of $AuCl_4^-$ may produce $AuCl_3^-$ and Cl atom in solution. The Cl atom in turn could cause abstraction of H-atom from the scavenger R−OCH_2CH_2OH, similarly as $OH^\bullet$. They are, therefore, able to reduce metal ions.

$$R{-}OCH_2CH_2{-}OH \xrightarrow{OH^\bullet} R{-}OCH_2CH^\bullet{-}OH + H_2O$$

$$R{-}OCH_2CH_2{-}OH \xrightarrow{H^\bullet} R{-}OCH_2CH^\bullet{-}OH + H_2$$

$$R{-}OCH_2CH^\bullet{-}OH + M^+ \rightarrow M + R{-}OCH_2CHO + H^+$$

The atoms are formed homogeneously throughout the solution. The binding energy between two transition metal atoms is higher than the atom−solvent bond energy.

The seeding effects described here will literally apply to other systems also, especially when the seed is generated as the important but first step of the gradual growth of the particles. It is shown how strongly the elementary processes during the growth of small seed particles are affected by the reducing power of reducing agents/nucleophiles. The selective shape-dependent growth of the particles during their successive development is now a challenging task and warrants further and extensive theoretical work. In our previous work,[16] the same type of seed particle development resulted in monometallic cubical copper, spherical silver, and nonspherical gold particles. This seed mediated development should be looked into from the point of surface energy of the particular seed particles for further crystal growth. The advantage of the photochemical method of reduction to produce size-controlled synthesis of gold nanoparticles has been described elsewhere.[17] This method has an advantage over wet chemical methods in which excess reducing agent may hamper the desired synthesis. Second, the rate of reaction is well known because the number of reducing equivalents generated by radiation is well defined and radiation is absorbed regardless of the presence of light-absorbing solutes and products.

In conclusion, the novelty of this two-step seed mediated preparation of bimetallic nanoparticles lies in its simplicity and simultaneous control of both size and shape of the particles without any use of capping agent or template. The seed mediated technique or its modified version may be useful for other systems of nanoparticles for producing particles of desired size.

References

(1) Aihira, N.; Torigoe, K.; Esumi, K. *Langmuir* **1998**, *14*, 4945.
(2) Itakura, T.; Torigoe, K.; Esumi, K. *Langmuir* **1995**, *11*, 4129.
(3) Link, S.; Wang, Z. L.; El-Sayed, M. A. *J. Phys. Chem. B* **1999**, *103*, 3529.
(4) Treguer, M.; de Cointet, C.; Remita, H.; Khatouri, J.; Mostafavi, M.; Amblard, J.; Belloni, J.; de Keyzer, R. *J. Phys. Chem. B* **1998**, *102*, 4310.
(5) de Cointet, C.; Mostafavi, M.; Khatouri, J.; Belloni, J. *J. Phys. Chem.* **1997**, *18*, 3512.
(6) Schmid, G.; Lehnert, A.; Malm, J.-O.; Bovin, J.-O. *Angew. Chem., Int. Ed. Engl.* **1991**, *30*, 874.
(7) Henglein, A. *J. Phys. Chem. B* **2000**, *104*, 2201.
(8) Pal, A. *Talanta* **1998**, *46*, 583.
(9) Henglein, A. *J. Phys. Chem.* **1993**, *97*, 5457.
(10) Belloni, J. *Curr. Opin. Colloid Interface Sci.* **1996**, *1*, 184.
(11) Mosseri, S.; Henglein, A.; Janata, E. *J. Phys. Chem. B* **1989**, *18*, 6791.
(12) Remita, S.; Archirel, P.; Mostafavi, M. *J. Phys. Chem. B* **1995**, *35*, 13198.
(13) Texier, I.; Remita, S.; Archirel, P.; Mostafavi, M. *J. Phys. Chem. B* **1996**, *30*, 12472.
(14) Belloni, J.; Mostafavi, M.; Remita, H.; Margnier, J.-L.; Delcourt, M.-O. *New J. Chem.* **1998**, 1239.
(15) Pal, T.; Ganguly, A.; Maity, D. *Anal. Chem.* **1986**, *58*, 564.
(16) Pradhan, N.; Jana, N. R.; Kaushik, M.; Pal, T. *Colloid. Surf. Technol.*, accepted.
(17) Kaushik, M.; Wang, Z. L.; Pal, T. *J. Photochem. Photobiol. A* **2001**.

NL0100264